Synergistic anticancer activity of doxorubicin and piperlongumine on DU-145 prostate cancer cells – The involvement of carbonyl reductase 1 inhibition

Kamil Piska[a,1], Paulina Koczurkiewicz[a,*,1], Dawid Wnuk[b], Elżbieta Karnas[b,c], Adam Bucki[d], Katarzyna Wójcik-Pszczoła[a], Marek Jamrozik[d], Marta Michalik[b], Marcin Kołaczkowski[d], Elżbieta Pękala[a]

[a] Department of Pharmaceutical Biochemistry, Faculty of Pharmacy, Jagiellonian University Medical College, Kraków, Poland
[b] Department of Cell Biology, Faculty of Biochemistry, Biophysics and Biotechnology, Jagiellonian University, Kraków, Poland
[c] Malopolska Centre of Biotechnology, Jagiellonian University, Krakow, Poland
[d] Department of Medicinal Chemistry, Faculty of Pharmacy, Jagiellonian University Medical College, Kraków, Poland

ARTICLE INFO

ABSTRACT

One of the causes of therapeutic failure of chemotherapy is cancer cell resistance. In the case of anthracyclines, many resistance mechanisms have been described. One of them assumes the role of carbonyl reductase 1 (CBR1), a cytosolic enzyme that is responsible for the biotransformation process of anthracyclines to less active, undesirable metabolites. Therefore, CBR1 inhibitors are considered for use as a chemosensitizing agents. In the present study, piperlongumine (PL), a *Piper longum* L. alkaloid that has previously been described as a CBR1 inhibitor, was investigated for its chemosensitizing properties in co-treatment with doxorubicin (DOX). The biotransformation process of DOX in the presence of PL was tracked using human cytosol fraction and LC-MS, then a molecular modeling study was conducted to predict the interaction of PL with the active site of the CBR1. The biological interaction between DOX and PL was investigated using DU-145 prostate cancer cells. Cytotoxic and antiproliferative properties of DOX and PL were examined, and the type and potency of interaction was quantified by Combination Index. The mechanism of the cell death induced by the agents was investigated by flow cytometry and the anti-invasive properties of the drugs were determined by monitoring the movement of individual cells. PL showed dose-dependent inhibition of DOX metabolism in cytosol, which resulted in less doxorubicinol (DOXol) metabolite being formed. The possible mechanism of CBR1 inhibition was explained through molecular modeling studies by prediction of PL's binding mode in the active site of the enzyme's crystal structure-based model. DOX and PL showed a synergistic antiproliferative and proapoptotic effect on cancer cells. Significant anti-invasive properties of the combination of DOX and PL were found, but when the drugs were used separately they did not alter the cancer cells' motility. Cell motility inhibition was accompanied by significant changes in cytoskeleton architecture. DOX and PL used in co-treatment showed significant synergistic anticancer properties. Inhibition of DOX metabolism by PL was found to be a mechanism that was likely to be responsible for the observed interaction.

1. Introduction

Anthracycline antibiotics are among the most frequently used drugs in clinical oncology. These nature-derived compounds are applied in treatment of solid cancers and hematological malignancies [42]. Although many new anthracyclines have been developed over the years, and many are clinically applied, classic drugs like doxorubicin (DOX), daunorubicin and epirubicin are still commonly applied in

chemotherapy regimens. Despite anthracyclines' high efficacy and broad spectrum of activity, a significant limitation of their use in therapy is the resistance of cancer cells, which reduces response to treatment in many subjects. Cancer cell resistance is a complex phenomenon and many molecular bases of its development have been proposed, one of which indicated the role of cytosolic reductase enzymes, including carbonyl reductases (CBRs) and aldo-keto reductases (AKRs). These enzymes are able to metabolize anthracyclines such as DOX to less active secondary alcohol metabolites such as doxorubicinol (DOXol) by reduction of the C13 carbonyl group on the side chain of the drug. Metabolites that are formed during biotransformation of anthracyclines are less toxic for tumor cells and their formation is one of the causes of resistance to therapy [35]. The expression of cytosolic reductases is significantly increased in response to treatment with anthracyclines [12]. The CBR/AKR-dependent rate of DOX reduction has been correlated with sensitivity of cells to DOX. This resistance mechanism plays a role not only in secondary resistance, but it is also important in native sensitivity of cells to drugs [2]. Therefore, CBR and AKR inhibitors have been considered as chemosensitizing agents that can overcome the decreased response to anthracycline therapy.

Piperlongumine (PL) is an amide alkaloid isolated from long pepper (*Piper longum* L. *Piperaceae*), an Ayurvedic medicinal plant which exhibits anticancer activity in both *in vitro* and *in vivo* models [4]. Its anticancer activity is associated with the generation of reactive oxygen species, induction of apoptosis in cancer cells, and a strong anti-invasive effect [19,36,41,44]. PL can also selectively kill numerous types of malignant cells without affecting normal ones [6,36]. Furthermore, PL does not show significant toxicity in rodents, while pharmacokinetic studies have indicated its high oral bioavailability [4,36]. It has a broad spectrum of molecular targets; however, it is also characterized as a CBR1 inhibitor [36], a predominant enzyme involved in the reduction of DOX to the less active metabolite, DOXol [21].

Taking into account the above facts, in the present study we focused our attention on the potential synergistic interaction of PL and DOX. Firstly, PL was evaluated using a cytosolic fraction as a potential inhibitor of the CBR1-mediated metabolism of DOX to DOXol. Then, crystal structure-based molecular docking was used to determine the binding mode of PL in the active site of the CBR1 enzyme. Finally, the activity of the PL and DOX combination was studied on the DU-145 prostate cancer cell line. The cells' viability, proliferation, induction of the apoptosis process, motility and cytoskeleton organization were evaluated. Our results proved that PL can interact with the active site of the carbonyl reductase enzyme, decrease the level of the secondary metabolite (DOXol), and act synergistically with DOX, thereby improving its anti-cancer properties.

2. Materials and methods

2.1. Influence of PL on the reductive metabolism of DOX

The reaction mixture contained DOX (Cayman; final concentration 20 μM), PL (Sigma Aldrich; 10, 20, 30, 40, 50 μM), human liver cytosol (2 mg of protein/ml), NADPH-regenerating system (Sigma Aldrich; $NADP^+$, glucose-6-phosphate, glucose-6-phosphate dehydrogenase in 0.1 M potassium phosphate buffer, pH 7.4) and 0.1M potassium phosphate buffer (pH 7.4). After 10 min of preincubation of cytosol with drugs at 37 °C, the NADPH-regenerating system was added to initiate the reaction. The incubation was carried out for 120 min at 37 °C and 350 rpm in a Thermomixer (Eppendorf). The reaction was terminated with ice-cold methanol. Daunorubicin hydrochloride (Cayman) was added as an internal standard. After centrifugation at 12,000 rpm for 10 min, the supernatant was collected and analyzed by UPLC-MS/MS. Control reactions were carried out in the absence of PL or NADPH-regenerating systems.

2.2. UPLC-MS/MS condition

The UPLC-MS/MS system consisted of a Waters ACQUITY® UPLC® (Waters Corporation, Milford, MA, USA) coupled to a Waters TQD mass spectrometer (electrospray ionization mode ESI-tandem quadrupole). Chromatographic separations were carried out using an Acquity UPLC BEH (bridged ethyl hybrid) C18 column; 2.1 × 100 mm, and 1.7 μm particle size. The column was maintained at 40 °C and eluted under gradient conditions using 95%–0% of eluent A over 10 min at a flow rate of 0.3 ml min-1. Eluent A was water/formic acid (0.1%, v/v); eluent B was acetonitrile/formic acid (0.1%, v/v). 10 μL of each sample was injected. Chromatograms were recorded using a Waters λ PDA detector. Spectra were analyzed in the 200–700 nm range with 1.2 nm resolution and a sampling rate of 20 points/s. MS detection settings of the Waters TQD mass spectrometer were as follows: source temperature 150 °C, desolvation temperature 350 °C, desolvation gas flow rate 600 L h-1, cone gas flow 100 L h-1, capillary potential 3.00 kV, cone potential 20 V. Nitrogen was used for both the nebulizing and the drying gas. The data were obtained in a scan mode ranging from 50 to 1000 *m/z* in 0.5 s time intervals; 8 scans were summed to get the final spectrum. Collision-activated dissociation (CAD) analyses were carried out with an energy of 20 eV, and all the fragmentations were observed in the source. The data acquisition software was MassLynx V 4.1 (Waters).

2.3. Molecular modeling

The molecular modeling studies involved the development of a computational model of carbonyl reductase 1 (CBR1) based on the experimental structure of the enzyme co-crystallized with hydroxy-PP (PDB ID: 1WMA) [40]. The structure was refined using Protein Preparation Wizard [29]. Water molecules and hetero groups other than hydroxy-PP and NADPH (dihydro-nicotinamide-adenine dinucleotide phosphate) were deleted and the energy of the whole system was minimized (OPLS3 force field). The model was tested throughout docking studies involving a variety of chemical classes of CBR1 orthosteric ligands, e.g. hydroxy-PP, which resulted in ligand RMSD = 0.3132 Å comparing to the position found in the 1WMA crystal complex. The obtained consistent binding modes of the reference compounds of experimentally proven affinity verified the accuracy of the crystal-based model [1,34]. Ligand structures were optimized using the LigPrep tool (OPLS3 force field), generating all possible protonation states in the pH range 7 ± 2 according to Epik. The centroid of the grid box was located on hydroxy-PP from 1WMA, while H-bond constraints were set on Ser139 and Tyr193 (at least one of them had to be matched). Flexible docking was carried out using default parameters of standard precision Glide (SP). The algorithm generated ligand conformations internally during the docking process by variating around acyclic torsions and sampling ring conformations. Post-docking minimization was performed to retrieve 5 low energy complexes for each ligand. The obtained poses were then evaluated based on glide gscore values and visual inspection. Glide, LigPrep and Protein Preparation Wizard were implemented in Small-Molecule Drug Discovery Suite (Schrödinger, Inc.), licensed for Jagiellonian University Medical College.

2.4. Cells and cell cultures

Human prostate cancer cell line DU-145 (ATCC, HTB-81™) was used in the study. The cells were cultured in standard conditions (37 °C, 5% CO_2) in DMEM/F-12 medium (Sigma-Aldrich), supplemented with 10% FBS (Gibco) and antibiotics (Sigma-Aldrich; 1% streptomycin/penicillin mixture).

2.5. Lactate dehydrogenase (LDH) cytotoxicity assay

Cells were seeded into a 96-well plate at a density of 5×10^3 cells

per well. After 24 h, DOX and PL were added separately or in combinations to final concentrations of 0.01; 0.05 and 0.1 μM for DOX, and 0.1, 0.5 and 1.0 μM for PL. After 24 h and 72 h incubations, plates were centrifuged (400 g, 5 min) and 100 μL of the supernatant was transferred into the corresponding 96-well plate. Subsequently, 100 μL of LDH-reaction mixture prepared according to the supplier's instructions was added to each well. Incubation was conducted in darkness for 30 min at room temperature. Next, absorbance was measured at 492 nm (A_{492}) using a multi-well plate reader (Spectra Max iD3, Molecular Devices). Cytotoxicity was determined as follows: cytotoxicity (%) = [(experiment A_{492} – negative control A_{492})/(positive control A_{492} – negative control A_{492})] x 100. The positive control was prepared by treating cells with Triton-X. The medium used in the LDH assay contained 1% FBS. Three independent experiments were performed for each condition.

2.6. Crystal violet proliferation assay

Cells were seeded into a 24-well plate at a density of 1×10^4 cells per well. After 24 h, DOX and PL were added separately or in combinations to the final concentrations used in the viability assays. After 24 and 72 h incubations, the cells were fixed for 15 min in a solution of formaldehyde in PBS (3.7%), washed with PBS and subsequently stained with 500 μL of 0.01% crystal violet solution for 10 min. The dye that stained the cells on the plates was eluted by 500 μL methanol solution (25% V/V) of citric acid (1.33% m/V) and sodium citrate (1.09% m/V), and the optical density of the extracted dye was read with a spectrophotometer at 540 nm (A_{540}). Inhibition of proliferation was calculated: inhibition of proliferation (%) = (1 – (experiment A_{540}/control A_{540})) x 100.

2.7. Combination index estimation

To quantify drug interaction, the Combination Index (CI) was estimated by the Chou-Talalay method using CompuSyn software (ComboSyn, Inc. NY, USA). CI < 1 indicates synergism, CI = 1 indicates additive interaction, and CI > 1 indicates antagonism [8].

2.8. Time-lapse monitoring of movement of individual cells

Cell movements were observed with an inverted Leica DMI6000B microscope with IMC optics at 37 °C and 5% CO_2 atmosphere. DU-145 cells were seeded into a 24-well plate at a density of 1×10^4 cells/cm^2. After 24 h the medium was replaced with a new one containing the agents, and time-lapse recording of cell movements was immediately performed. The cell trajectories were constructed from 40 subsequent centroid positions and photographed at 15-min time intervals for 480 min. They were presented in circular diagrams with the starting point of each trajectory at the plot center. The parameters characterizing cell locomotion were calculated as described previously with the Hiro program [28]. For each data point measured, 40 cells were analyzed. Pre-apoptotic and apoptotic cells were discriminated by morphology and their trajectories were not considered for statistical analysis. Three independent experiments were performed for each condition.

2.9. Influence of PL and DOX on apoptosis process

2.9.1. Cell morphology analysis

DU-145 cells were seeded into 6-well culture plates at a density of 5×10^3 cells/cm^2. After 24 and 72 h of incubation with agents, the morphology of the cells was analyzed in phase contrast with an Olympus inverted research microscope (model IX81) equipped with MicroPublisher 3.3 RTV, a High-Resolution IEEE FireWire™ Digital CCD Color Camera (Qimaging), and cellSens Standard 1.12 software.

2.9.2. Flow cytometry analysis

DU-145 cells were seeded into 6-well culture plates at a density of 5×10^3 cells/cm^2. After 24 h of culture, cells were incubated with analyzed agents for 48 h. Next, cells were washed with PBS, trypsinized, centrifuged (300 g, 4 min) and counted with a Bürker's chamber. Subsequently, cells were stained with an Annexin V Apoptosis Detection Kit (BD Bioscience) according to a modified manufacturer's protocol. Briefly, cells (1×10^5) were resuspended in a 1 x Binding Buffer to the final concentration of 1×10^6 cells/ml. Then, FITC-conjugated Annexin V and 7-AAD nuclear dye were added for 15 min in RT. Flow cytometric analysis of stained cells was performed with BD LSRFortessa cytometer and BD FACS Diva Software ver. 8.1 (Becton Dickinson). 1×10^4 of the cells were analyzed in each experiment. Three independent experiments were performed.

2.9.3. Immunoblotting

The supernatant was harvested from all experimental conditions; the cells were washed with cold PBS and trypsinized. Next, the supernatant and (apoptotic/necrotic) cells were centrifuged (300 g. 5 min); the cells were disrupted by exposure to lysing buffer (165 mM TrisHCl; 150 mM NaCl; 0,3 mM sodium azide; 1% Triton X100; H_2O) for 10 min in ice and homogenized with a protease inhibitor cocktail (Merck Milipore). The lysates were cleared by centrifugation (15 min, 1500 g, 4 °C) and protein concentration was determined using the Bradford method. Protein mixtures (20 μg per well) were separated by 10% SDS-polyacrylamide gel electrophoresis and transferred into PVD membranes (BioRad). Blots on PVD membranes were washed with TBST (10 mM Tris–HCl, 150 mM NaCl, 0.05% Tween-20), blocked with 3% skimmed milk (in TBST) for 45 min, and incubated with the appropriate primary antibody at the recommended dilutions: polyclonal rabbit anti-Bax IgG (Cell Signalling) and antibodies from the Apoptosis Antibody Sampler Kit (Cell Signalling, #9915). After overnight incubation (4 °C), membranes were washed with TBST and incubated with anti-rabbit IgG and anti-mouse IgG/IgM antibodies conjugated to horseradish peroxidase (1:3000), treated with Luminata Crescendo Western HRP Substrate (Merck Milipore), and visualized by chemiluminescence in the MicroChemi imaging system (SNR Bio-Imaging Systems, Jerusalem, Israel).

2.10. The influence of PL and DOX on the cell cytoskeleton

Analyses of actin cytoskeleton and vinculin architecture in DU-145 were performed on samples (cells seeded in ibidi μ-plate; 82401) fixed with 3.7% formaldehyde in PBS with Ca^{2+}, Mg^{2+} ions, permeabilized with 0.1% Triton X-100. Cells were stained with Alexa Fluor® 568 phalloidin as a manufacturer protocol (Molecular Probes, Life Technologies) and Hoechst 33258 (1 μg/ml; Sigma-Aldrich), mounted on basic slides in a fluorescent mounting medium (DAKO), and analyzed with a Leica DMI6000 B inverted microscope (Leica Microsystems GmbH, Wetzlar, Germany).

2.11. Statistical analysis

One-way analysis of variance (ANOVA) with a post-hoc Tukey's test was used to determine statistical significance. p values less than 0.05 were considered statistically significant. Statistical analyses were performed with the use of Statistica software.

3. Results

3.1. The influence of PL on DOX biotransformation

DOX incubated with cytosol and the NADPH-regenerating system resulted in the formation of one metabolite, DOXol, which was identified by comparison of retention time and fragmentation pattern against an analytical reference sample. After a 2-h incubation, 25.09% of DOX
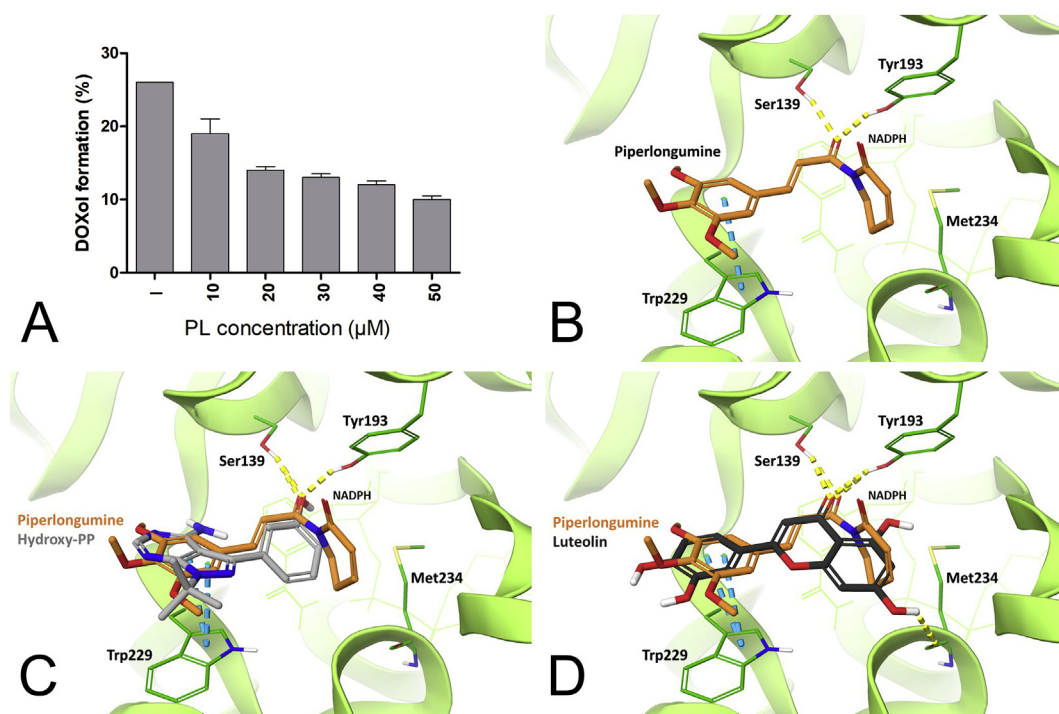
Fig. 1. Doxorubicin (DOX) metabolism in the presence of piperlongumine (PL)(A). The predicted interactions of piperlongumine with the catalytic domain of CBR1 (B); displayed together with hydroxy-PP (C) and luteolin (D). Impact of PL on metabolism of DOX in cytosolic fraction. DOX and PL were incubated with cytosol in increasing concentrations of PL, in the presence of the NADPH-regenerating system. The graph shows the relative amounts of doxorubicinol (DOXol) resulting from the biotransformation of DOX in the presence of PL in comparison to control. Values represent means ± SD. Each experiment was done three times independently (A). The most evident binding mode of PL in the active site of CBR1 is characterized by the presence of three main favorable interactions: hydrogen bonds (H-bonds) between carbonyl group of the prop-2-enoyl linker and two residues - Ser139 and Tyr193, as well as an aromatic interaction (π-π) with Trp229 (B). The same binding mode was observed for the reference compounds – hydroxy-PP (C) and luteolin (D). Crucial amino acid residues engaged in ligand binding throughout H-bonds (dotted yellow lines) and π-π stacking (dotted blue lines) are represented as thick sticks. NADPH – dihydro-nicotinamide-adenine dinucleotide phosphate (displayed as sticks). (For interpretation of the references to colour in this figure legend, the reader is referred to the Web version of this article.)

was metabolized to DOXol. The stability of DOX in the presence of PL significantly increased, as was observed by the decreased level of DOXol compared to the control (without PL) (Fig. 1A). The observed effect was dose dependent; the best stability was determined at 50 μM PL when formation of DOXol reached 9.46%, which means 62.3% inhibition of biotransformation.

3.2. Molecular modeling

A putative binding mode of PL in the active site of CBR1 was elucidated throughout docking to the target protein model, as represented by the optimized crystallographic structure 1WMA. The crucial interactions in the active site of the enzyme, which are in line with those observed for other known inhibitors [1,34], are presented in Fig. 1. The molecule of PL was docked in the substrate-binding site, where NADPH was complexed in the crystal structure. The 5,6-dihydropyridin-2(1H)-one moiety was located in the vicinity of the nicotinamide ribose moiety of NADPH and amino acids involved in the catalytic reaction [10]. The molecule was anchored by the hydrogen bond between the carbonyl group of the prop-2-enoyl linker and the hydroxy group of Ser139, which allowed for interaction with Tyr193, the amino acid residue that takes part in the enzymatic catalysis. Such orientation of PL, distinguished by the interaction with the amide's, not the lactam's carbonyl group, is authenticated by the possibility of forming an aromatic interaction (π-π stacking) between the trimethoxyphenyl moiety and Trp229 (Fig. 1B). Such a binding mode was characterized by better structure geometry alignment with the reference compounds: hydroxy-PP (Fig. 1C) and luteolin (Fig. 1D). Distances between the predicted bioactive conformations of ligands and residues involved in the molecular recognition within CBR1 catalytic domain are presented in

Table 1.

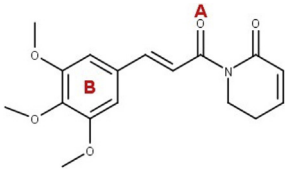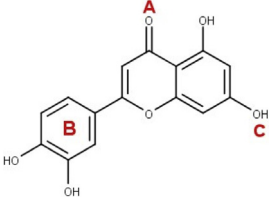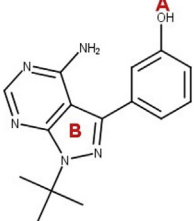### 3.3. The effect of DOX, PL, and DOX + PL on the viability of DU-145 cells

For further synergy analysis, an LDH viability assay was performed to examine non-toxic concentrations of the analyzed compounds. Neither DOX (in concentrations 0.01/0.05/0.1 μM) nor PL (in concentrations 0.1/0.5/1 μM) induced a meaningful cytotoxic effect in DU-145 cells after 24 h (Fig. 2A). Moderate cytotoxic effect of PL in concentration of 1 μM was observed after 72 h. However, combined treatment with DOX and PL resulted in an increase of cytotoxicity level after 72 h of incubation. The combination index (CI) for each combination is presented in Fig. 2E. CI for most combinations was less than 0.9, which indicates synergistic interaction between DOX and PL, but CI also reaches very small values, which classified the synergy as strong (< 0,3).

3.4. Effect of DOX, PL and DOX + PL on proliferation of DU-145 cells

The influence of agents on DU-145 cell proliferation was studied using a crystal violet assay. The cytostatic effect of PL was evident and dose-dependent, while DOX did not induce significant growth inhibition of DU-145 cells. PL used in highest concentration (1 μM) decreased proliferation by more than 60% after 72 h of incubation (Fig. 2C). However, the combined treatment (DOX + PL) resulted in an increase of the cytostatic properties of the drugs, even in ineffective concentrations of PL and DOX when used alone (Fig. 2D). The Combination Index (Fig. 2E) indicated strong and very strong synergies for some combinations.

Table 1
Distances between key amino acid residues and significant moieties of CBR1 inhibitors measured in ligand-protein complexes obtained in docking simulations.

Compound	A		B	C
	Ser139 (H-bond)	Tyr193 (H-bond)	Trp229 (π- π)	Met234 (H-bond)
	1,98 Å	1,81 Å	3,98 Å	–
	1,92 Å	2,28 Å	4,17 Å	2,56 Å
	2,08 Å	–	3,84 Å	–

3.5. The effect of DOX, PL, and DOX + PL on the apoptosis process

To evaluate the apoptosis process after PL, DOX, and PL + DOX treatment, cellular morphology observation, flow cytometry analysis (cells stained with Annexin V/7-AAD), and Western blot analysis (level of PARP, Casp3 and Bax protein) were performed. The results indicated that when applied at non-cytotoxic concentrations, the combination of PL and DOX induces an apoptotic response in DU-145 cells. The analyses of cellular morphology after 24 h of incubation in the presence of PL + DOX resulted in the appearance of morphologically altered cells which displayed blebs reminiscent of apoptotic bodies, as well as some necrotic features (Fig. 3A and B). Flow cytometry analysis performed after 48 h of incubation showed that PL or DOX alone did not induce apoptosis, whereas their combination slightly increased the fraction of Annexin V positive cells (Fig. 3C). The level of cleaved PARP and Caspase 3 proteins (their active forms) in treated cells (Fig. 3D) confirmed the synergistic character of the pro-apoptotic effects of PL and DOX in DU-145 populations. A significantly increased level of both proteins in DU-145 cells treated with the PL/DOX cocktails was observed.

3.6. The effect of DOX, PL, and DOX + PL on DU-145 cell migration and cytoskeleton organization

To evaluate the effect of PL, DOX, and PL/DOX on cancer cell migration, time-lapse monitoring of the movement of individual cells was performed. Neither agent significantly inhibited the migration DU-145 cancer cells when applied alone at concentrations of 0.5 and 0.1 μM. The magnitude of this attenuation was highest in the presence of PL/DOX (Fig. 4A). Both agents used together synergistically reduced the length of the cells' trajectory and the speed of their movement. The effects of PL/DOX on DU-145 motility were paralleled by changes in cytoskeleton architecture, i.e. partial disintegration and reduced focal adhesion contact (Fig. 4B).

4. Discussion

The incidence of cancer is increasing every year. According to analysis performed by GLOBOCAN the number of new cases will double over the next five years. Despite the huge progress that has been made in oncology over the years, patient mortality is still high. The effectiveness of chemotherapy is burdened by numerous side effects [5]. Due to the adverse effects of chemotherapy, in recent years the idea of sensitizing cancer cells to chemotherapeutics has been intensively investigated. Numerous studies have shown that combining chemotherapeutics with phytochemicals can decrease their effective doses, limit toxicity, and improve selectivity [7,23,24,26,31]. Several mechanisms of chemosensitization have been found, the most studied being the inhibition of ABC transporters. The efflux function of ABC transporters reduces the concentration of intracellular drugs, leading to decreased anti-cancer action. This mechanism also affects the activity of anthracyclines. The clinical efficacy of DOX has been found to be dependent on the expression of ABCB1 and other transporters in cancer cells [37]. However, the use of ABC transporter inhibitors did not improve the efficacy of drugs in clinical trials and was associated with increased cardiac toxicity [9]. Therefore, searching for a novel mechanism of resistance is extremely important. Inhibition of CBR1, which leads to decreased biotransformation of anthracyclines to their less active metabolites, has been shown to be an effective way to increase anticancer activity of anthracyclines *in vitro* and *in vivo*. A promising chemosensitizing effect against anthracyclines was achieved by using several agents with CBR1-inhibiting properties, including epigallocatechin gallate, curcumin, berberine, and 23-hydroxybetulic acid [16–18,46]. These compounds increased anthracyclines' cytotoxicity and/or cytostatic action against cancer cells.

During the search for a new inhibitor of CBR1, our attention was drawn to piperlongumine (PL), an alkaloid isolated from *Piper longum* [36]. PL cytotoxicity was proved for various tumor cells using numerous *in vitro* and *in vivo* studies. Its effect is based on the induction of programmed cell death, largely via apoptosis, but also via necroptosis and autophagy, anti-invasive action and inhibition of cancer cell
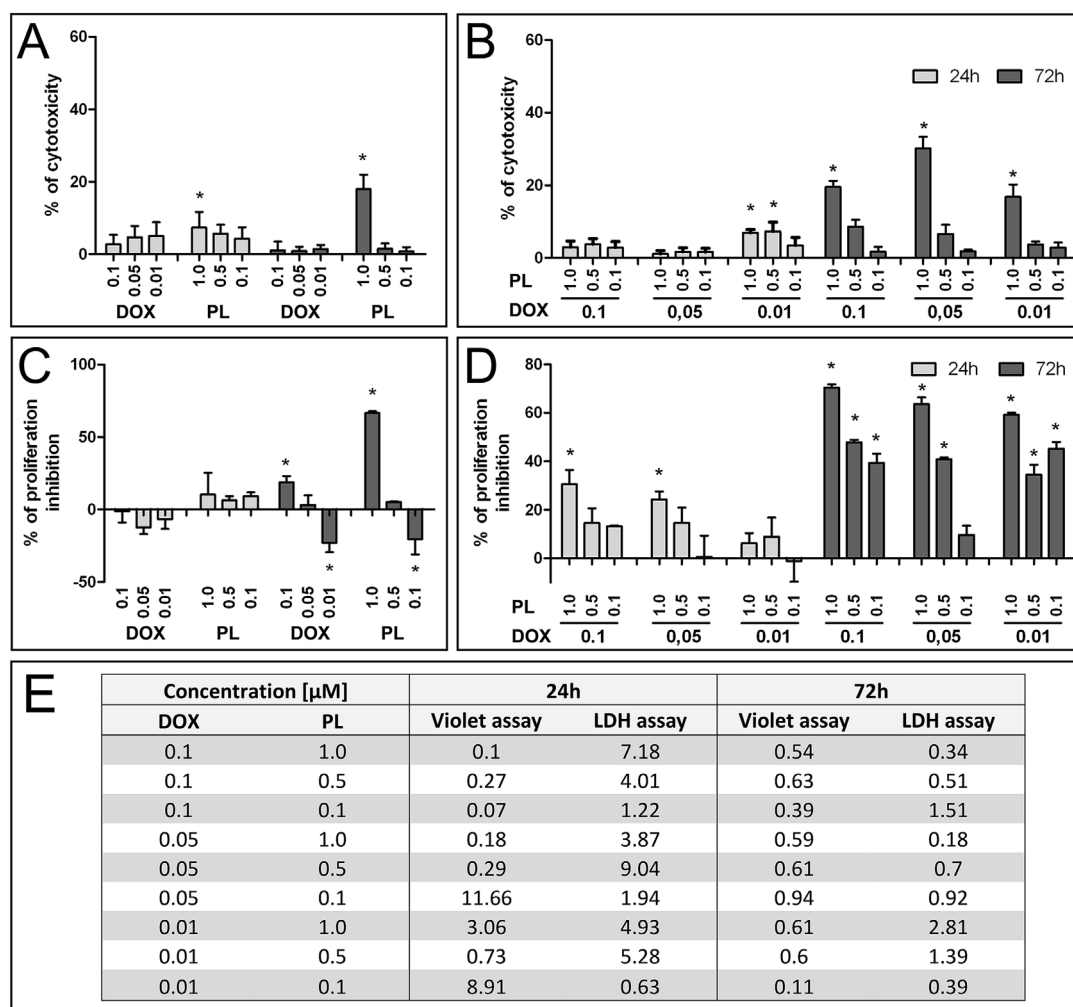
Concentration [μM]		24h		72h	
DOX	PL	Violet assay	LDH assay	Violet assay	LDH assay
0.1	1.0	0.1	7.18	0.54	0.34
0.1	0.5	0.27	4.01	0.63	0.51
0.1	0.1	0.07	1.22	0.39	1.51
0.05	1.0	0.18	3.87	0.59	0.18
0.05	0.5	0.29	9.04	0.61	0.7
0.05	0.1	11.66	1.94	0.94	0.92
0.01	1.0	3.06	4.93	0.61	2.81
0.01	0.5	0.73	5.28	0.6	1.39
0.01	0.1	8.91	0.63	0.11	0.39

Fig. 2. Effect of DOX and PL on cytotoxicity and proliferation of DU-145 cells. Cells were cultured in standard condition in the presence of DOX or PL used alone (A,C) and cocktails of DOX + PL (B,D). After 24 and 72 h LDH assay was performed to measured cellular viability as well as crystal violet proliferation test to measure cells proliferation rate. Graphs A, B present cytotoxicity (%) of PL and DOX used alone (A) and in combination (B). Graphs C, D present inhibition of proliferation (%) of PL and DOX used alone (C) and in combination (D). Values represent means ± SD. Each experiment was done three times independently; *statistically significant vs. control at p < 0,05. (E) Combination Index (CI) values for DOX and PL combinations in DU 145 cells. CI values were calculated using the CompuSyn software. CI values < 0.9 indicate synergism; CI = 1, additivity; and CI > 1.1, antagonism.

proliferation [4]. PL showed selective activity, without apparent toxicity in normal cells. Furthermore, PL has excellent oral bioavailability, inhibits tumor growth in rodents, and presents only weak systemic toxicity. Moreover, the literature contains reports about the potential inhibitory properties of PL against CBR1; however, this phenomenon has not yet been clarified [36]. Considering the anti-cancer activity of PL and its potential ability to inhibit the enzyme that is responsible for DOX metabolism and resistance, we decided to investigate the possible interaction between PL and DOX in the context of anticancer activity. Firstly, the metabolism of DOX in the presence of PL was investigated using human liver cytosol, in which CBR1 was found to be a predominant DOX reductase [21]. Incubation of DOX with cytosol resulted in partial metabolism of DOX to non-cytotoxic metabolite DOXol. Depending on the dose, the addition of PL to the reaction mixture ameliorated the stability of DOX, thus altering the rate of undesirable metabolite DOXol formation. When we observed that the level of DOXol formation during DOX metabolism was lower in the presence of PL, we were fairly confident that PL can interact with CBR1, therefore we decided to predict binding mode of PL in CBR1 using molecular modeling. The outcomes constantly indicated a favorable binding mode of PL, reflected by its interactions with the active site residues that are common for the previously described inhibitors [1,34]. These results

indicated the possibility of PL to act through the CBR1-dependent mechanism. However, further studies including recombinant anthracycline-metabolizing enzymes are required to completely characterize the molecular mechanisms of the agents' interaction with other cytosolic reductases of anthracyclines, i.e. AKR1C3, AKR1A1, or CBR3 [35].

In the present study, PL was found to exert synergistic properties with DOX in relation to the processes involved in cancer cell promotion and progression. Synergistic cytostatic, proapoptotic and anti-invasive effects of PL + DOX were observed against human prostate cancer cells (DU-145). The synergistic cytotoxic effect was achieved mainly for the highest concentrations of both agents, while synergistic cytostatic properties were found for the majority of tested combinations of DOX and PL concentrations. Piperlongumine and its structural analogues have previously been considered for use as tubulin-destabilizing agents that effectively inhibit MCF-7 cancer cell proliferation [30]. However only a few reports described a chemosensitizing action of PL used in combination with other agents on growth inhibition of cancer cells. PL enhanced the therapeutic effects of gemcitabine on pancreatic cancer, possibly through the modulation of NF-κB- and NF-κB-regulated gene products [43]. The process of apoptosis not only inhibits cancer progression but also leads to the elimination of cells that are resistant to therapeutic agents. Evaluation of proapoptotic activity is a significant
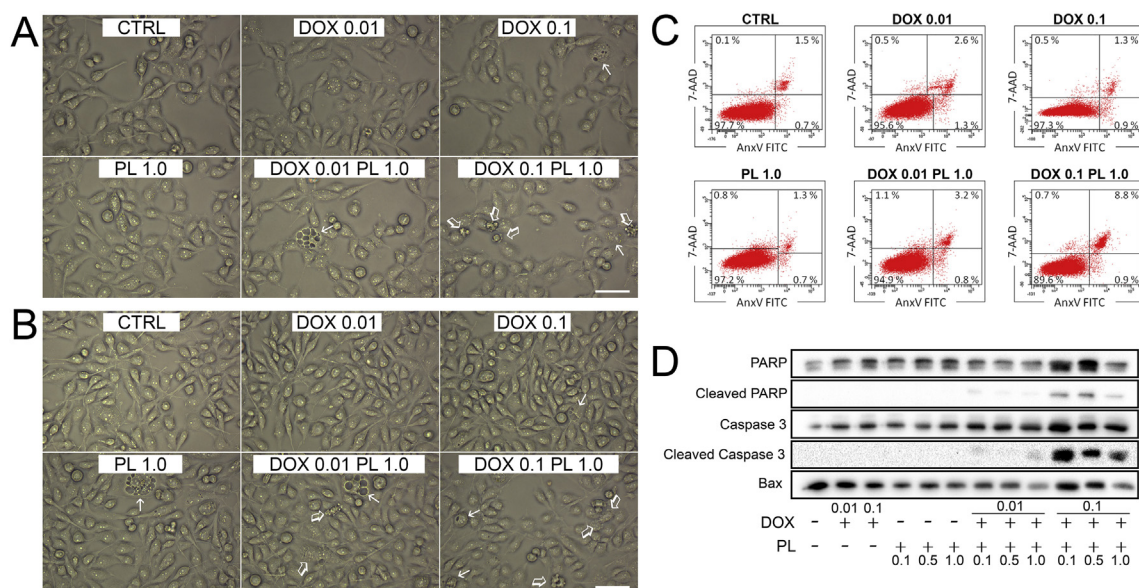
Fig. 3. Effect of DOX and PL on apoptosis process of DU-145 cells. Cells were cultured for 24 h (A) or 48 h (B, C) in PL, DOX, or PL + DOX supplemented medium and then cellular morphology was determined (A, B) and apoptotic cells were identified by flow cytometry (C). Representative dot plots of Anx V/7-AAD-stained DU-145 cells. The percentage of cells in each quadrant is indicated. At least 10,000 cells were counted for each experiment. Each experiment was done three times. Effect of PL- DOX- PL + DOX-on the expression of protein involved in apoptosis signal transduction in prostate cancer DU-145 cells (D). Cells were incubated with PL + DOX-for 72 h and protein levels was assessed by Western blot analysis as described in Materials and methods.

goal in cancer research aimed at identifying compounds that selectively affect cancer cells [11]. Piperlongumine and doxorubicin used alone have been described as proapoptotic agents in numerous studies [14,39,41]. We showed that co-treatments of PL and DOX are associated with induction of apoptosis in DU-145 cells. While only a slightly proapoptotic effect on DU-145 cells was observed for PL and DOX used alone, after DOX + PL treatment increased changes in cellular morphology evident for apoptosis were observed. Flow cytometry analysis showed an increasing number of Annexin V positive cells, and the level of apoptotic protein (Caspase 3 and PARP) was also higher. One study showed that CBR1 inhibition was related to an increase of DOX-related apoptosis. Hanušová et al. indicated increased apoptosis after

combination of DOX with oracin, an isoquinoline derivative, in the MCF-7 breast cancer cell line [15]. Similar intensification of the apoptosis process is also observed during combination treatment of anthracyclines with ABC inhibitors [22]. PL potentialized anticancer activity of several other cytostatic drugs, which may be the result of many molecular targets being affected. PL reduced bortezomib resistance in multiple myeloma cells (MM). In a disseminated MM mouse model, piperlongumine prolonged the survival of tumor-bearing mice without causing any obvious toxicity. PL has been shown to inhibit the STAT3 signal pathway by binding directly to the STAT3 Cys712 residue [45]. Furthermore, a low dose of PL and cisplatin or paclitaxel combinations had a synergistic antigrowth and proapoptotic effect on
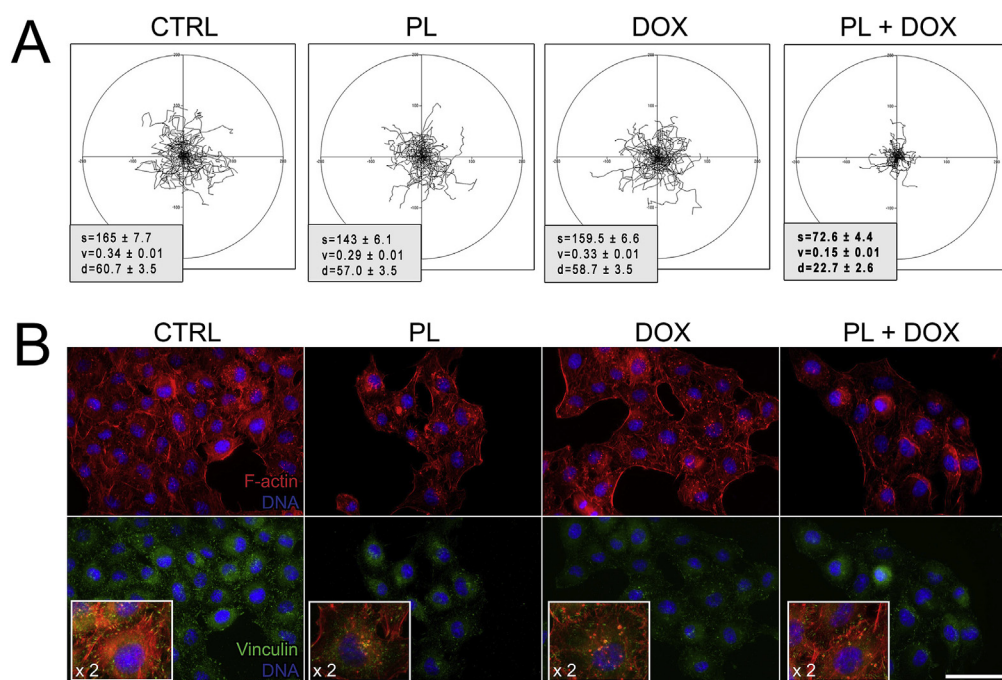

Fig. 4. Effect of DOX, PL and DOX + PL on actin cytoskeleton architecture and motility of DU-145 cells. Cells were seeded at density 1×10^4 cells/cm². After 24 h medium was replaced by medium without PL or DOX (control), medium containing PL alone in concentration 0.5 μM, DOX alone in concentration 0.1 μM, or medium containing cocktail of PL + DOX (0.5 + 0.1 μM). Time laps analyses of single cells movement were conducted (A), paralleled by fluorescent staining of actin cytoskeleton and vinculin (B). Circular diagrams present cell trajectories with the starting point of each trajectory situated at the plot center. Each experiment was done three times. (s = total length of cell movement [μm], v = average speed of movement [μm/min], d = total length of displacement [μm]).

human ovarian cancer cells [14]. PL can also improve the effects of the anti-cancer drug docetaxel by enhancing its oral bioavailability in rats and increasing cytotoxicity in a breast cancer cells model [32]. PL in combination with pancratistatin has been shown to be effective in reducing cancer cell growth in physiologically more relevant three-dimensional spheroid cell cultures. This enhanced effect has been found to be dependent on the generation of reactive oxygen species [27]. For more insight into the anti-cancer potential of the PL + DOX combination, we further concentrated on its effect on cancer cell motility and cytoskeleton organization, both of which may be of great importance regarding the ability of cancer cells to metastasis. At a selected concentration, PL and DOX used separately did not affect the movement of DU-145 cells. However, when these compounds were used in combination, we observed a significant decrease of all cells' motility parameters, i.e. the length of cells' trajectory, speed of movement, and length of displacement. This implies that the PL + DOX combination exerts a strong anti-invasive effect on prostate cancer cells, which may have significance in the prevention of metastasis and treatment of prostate cancer. Because cell movement is regulated by actin cytoskeleton dynamics, we further focused on the impact of PL/DOX on cytoskeleton organization. A more profound disintegration of actin microfilament bundles and a significant decrease of vinculin-positive focal adhesion plaques could also be observed for the PL + DOX combination. So far, PL has predominantly been investigated for its anti-invasive activity while, only an one study have described the anti-invasive potential of PL when used in co-treatment with other agents – with docetaxel [32]. PL alone has been shown to significantly suppress the motility of bladder cancer cells, prominently reduce lamellipodia formation, and decrease F-actin intensity in bladder cancer cells [25]. Furthermore, PL attenuates the expression of IL-6, IL-8, MMP-9, and ICAM-1, and decreases cell-to-matrix adhesion and invasiveness properties of prostate cancer cells [13].

5. Conclusions

At concentrations at which the individual components were non-cytotoxic, the cytostatic, pro-apoptotic and anti-invasive activities of PL and DOX cocktails demonstrate that such a combined treatment can be an advantageous cancer treatment that is ineffective when chemotherapeutics alone are used. This phenomenon was observed in the case of prostate cancer, in which DOX is clinically used [33]. Hence, the results of this study are encouraging for further research that considers PL as a chemosensitizing agent in DOX treatment. In this study, the synergy between DOX and PL was attributed to the CBR1-inhibition properties of PL. However, this mechanism does not exclude the involvement of the other mechanism than CBR1 inhibition. Previously, Kang and Yan indicated the ability of PL to reverse DOX resistance through the PI3K-Akt pathway [20]. Also, the inhibition of drug efflux out of cells was observed after treatment with PL [32]. Raj et al. described inhibition of GSTπ1 by PL, an enzyme which is involved in DOX resistance in cancer [36,38]. Therefore, explaining the interaction between PL and DOX may not be possible through only one mechanism. Moreover, this may become a novel approach to treat cancer resistance by affecting not only ABC-mediated drug efflux, but also CBR1-mediated metabolism. Simultaneously impacting two independent mechanisms associated with cancer resistance may be a promising strategy that is better than suppressing only one cancer resistance pathway.

Conflicts of interest

Authors declare no conflict of interest.

Acknowledgments

Appendix A. Supplementary data

Supplementary data to this article can be found online at https://doi.org/10.1016/j.cbi.2019.01.003.

References

[1] Y. Arai, S. Endo, N. Miyagi, N. Abe, T. Miura, T. Nishinaka, T. Terada, M. Oyama, H. Goda, O. El-Kabbani, A. Hara, T. Matsunaga, A. Ikari, Structure-activity relationship of flavonoids as potent inhibitors of carbonyl reductase 1 (CBR1), Fitoterapia 101 (2015) 51–56 https://doi.org/10.1016/j.fitote.2014.12.010.

[2] O.S. Bains, A. Szeitz, J.M. Lubieniecka, G.E. Cragg, T.a Grigliatti, K.W. Riggs, R.E. Reid, A correlation between cytotoxicity and reductase-mediated metabolism in cell lines treated with doxorubicin and daunorubicin, J. Pharmacol. Exp. Therapeut. 347 (2013) 375–387 https://doi.org/10.1124/jpet.113.206805.

[4] D.P. Bezerra, C. Pessoa, M.O. De Moraes, N. Saker-Neto, E.R. Silveira, L.V. Costa-Lotufo, Overview of the therapeutic potential of piplartine (piperlongumine), Eur. J. Pharm. Sci. 48 (3) (2013) 453–463, https://doi.org/10.1016/j.ejps.2012.12.003.

[5] D. Cappetta, A. De Angelis, L. Sapio, L. Prezioso, M. Illiano, F. Quaini, F. Rossi, L. Berrino, S. Naviglio, K. Urbanek, Oxidative stress and cellular response to doxorubicin: a common factor in the complex milieu of anthracycline cardiotoxicity, Oxid. Med. Cell. Longev. 2017 (2017), https://doi.org/10.1155/2017/1521020.

[6] Y. Chen, J.M. Liu, X.X. Xiong, X.Y. Qiu, F. Pan, D. Liu, S.J. Lan, S. Jin, S. Bin Yu, X.Q. Chen, Piperlongumine selectively kills hepatocellular carcinoma cells and preferentially inhibits their invasion via ROS-ER-MAPKs-CHOP, Oncotarget 6 (2015), https://doi.org/10.18632/oncotarget.3444.

[7] Z. Chen, C. Huang, T. Ma, L. Jiang, L. Tang, T. Shi, S. Zhang, L. Zhang, P. Zhu, J. Li, A. Shen, Reversal effect of quercetin on multidrug resistance via FZD7/β-catenin pathway in hepatocellular carcinoma cells, Phytomedicine 43 (2018) 37–45 https://doi.org/10.1016/j.phymed.2018.03.040.

[8] T.C. Chou, Drug combination studies and their synergy quantification using the chou-talalay method, Cancer Res. 70 (2) (2010) 440–446 https://doi.org/10.1158/0008-5472.CAN-09-1947.

[9] F.S. Chung, J.S. Santiago, M.F.M. De Jesus, C.V. Trinidad, M.F.E. See, Disrupting P-glycoprotein function in clinical settings: what can we learn from the fundamental aspects of this transporter? Am. J. Cancer Res. 6 (8) (2016) 1583–1598.

[10] C. Filling, K.D. Berndt, J. Benach, S. Knapp, T. Prozorovski, E. Nordling, R. Ladenstein, H. Jörnvall, U. Oppermann, Critical residues for structure and catalysis in short-chain dehydrogenases/reductases, J. Biol. Chem. 277 (2002) 25677–25684 https://doi.org/10.1074/jbc.M202160200.

[11] D. Finlay, P. Teriete, M. Vamos, N.D.P. Cosford, K. Vuori, Inducing death in tumor cells: roles of the inhibitor of apoptosis proteins, F1000Research 6 (2017) 587 https://doi.org/10.12688/f1000research.10625.1.

[12] M. Gavelová, J. Hladíková, L. Vildová, R. Novotná, J. Vondráček, P. Krčmář, M. Machala, L. Skálová, Reduction of doxorubicin and oracin and induction of carbonyl reductase in human breast carcinoma MCF-7 cells, Chem. Biol. Interact. 176 (2008) 9–18 https://doi.org/10.1016/j.cbi.2008.07.011.

[13] S. Ginzburg, K.V. Golovine, P.B. Makhov, R.G. Uzzo, A. Kutikov, V.M. Kolenko, Piperlongumine inhibits NF-??B activity and attenuates aggressive growth characteristics of prostate cancer cells, Prostate 74 (2014) 177–186 https://doi.org/10.1002/pros.22739.

[14] L.H. Gong, X.X. Chen, H. Wang, Q.W. Jiang, S.S. Pan, J.G. Qiu, X.L. Mei, Y.Q. Xue, W.M. Qin, F.Y. Zheng, Z. Shi, X.J. Yan, Piperlongumine induces apoptosis and synergizes with cisplatin or paclitaxel in human ovarian cancer cells, Oxid. Med. Cell. Longev. (2014) 2014 https://doi.org/10.1155/2014/906804.

[15] V. Hanušová, V. Králová, L. Schröterov, L. Trilecová, A. Pakostová, L. Skálov, The effectiveness of oracin in enhancing the cytotoxicity of doxorubicin through the inhibition of doxorubicin deactivation in breast cancer MCF7 cells, Xenobiotica 40 (2010) 681–690 https://doi.org/10.3109/00498254.2010.508821.

[16] G. Hao, Y. Yu, B. Gu, Y. Xing, M. Xue, Protective effects of berberine against doxorubicin-induced cardiotoxicity in rats by inhibiting metabolism of doxorubicin, Xenobiotica 45 (2015) 1024–1029 https://doi.org/10.3109/00498254.2015.1034223.

[17] J. Hintzpeter, J. Hornung, B. Ebert, H.J. Martin, E. Maser, Curcumin is a tight-binding inhibitor of the most efficient human daunorubicin reductase - carbonyl reductase 1, Chem. Biol. Interact. 234 (2015) 162–168 https://doi.org/10.1016/j.cbi.2014.12.019.

[18] W. Huang, L. Ding, Q. Huang, H. Hu, S. Liu, X. Yang, X. Hu, Y. Dang, S. Shen, J. Li, X. Ji, S. Jiang, J.O. Liu, L. Yu, Carbonyl reductase 1 as a novel target of (-)-epigallocatechin gallate against hepatocellular carcinoma, Hepatology 52 (2010) 703–714 https://doi.org/10.1002/hep.23723.

[19] H.O. Jin, Y.H. Lee, J.A. Park, H.N. Lee, J.H. Kim, J.Y. Kim, B.R. Kim, S.E. Hong, H.A. Kim, E.K. Kim, W.C. Noh, J.Il Kim, Y.H. Chang, S.Il Hong, Y.J. Hong, I.C. Park, J.K. Lee, Piperlongumine induces cell death through ROS-mediated CHOP activation and potentiates TRAIL-induced cell death in breast cancer cells, J. Canc. Res. Clin. Oncol. 140 (2014) 2039–2046 https://doi.org/10.1007/s00432-014-1777-1.

[20] Q. Kang, S. Yan, Piperlongumine reverses doxorubicin resistance through the PI3K/Akt signaling pathway in K562/A02 human leukemia cells, Exp. Ther. Med. 9 (2015) 1345–1350 https://doi.org/10.3892/etm.2015.2254.

[21] N. Kassner, K. Huse, H.J. Martin, U. Gödtel-Armbrust, A. Metzger, I. Meineke, J. Brockmöller, K. Klein, U.M. Zanger, E. Maser, L. Wojnowski, Carbonyl reductase 1 is a predominant doxorubicin reductase in the human liver, Drug Metab. Dispos. 36 (2008) 2113–2120 https://doi.org/10.1124/dmd.108.022251.

[22] S.A. Khaleel, A.M. Al-Abd, A.A. Ali, A.B. Abdel-Naim, Didox and resveratrol

sensitize colorectal cancer cells to doxorubicin via activating apoptosis and ameliorating P-glycoprotein activity, Sci. Rep. 6 (2016), https://doi.org/10.1038/srep36855.

[23] P. Koczurkiewicz, E. Kowolik, I. Podolak, D. Wnuk, K. Piska, A. Łabędź-Masłowska, K. Wójcik-Pszczoła, E. Pękala, J. Czyż, M. Michalik, Synergistic cytotoxic and anti-invasive effects of mitoxantrone and triterpene saponins from lysimachia ciliata on human prostate cancer cells, Planta Med. 82 (2016), https://doi.org/10.1055/s-0042-117537.

[24] P. Koczurkiewicz, I. Podolak, K.A. Wójcik, A. Galanty, Z. Madeja, M. Michalik, J. Czyz, Lclet 4 enhances pro-apoptotic and anti-invasive effects of mitoxantrone on human prostate cancer cells - in vitro study, Acta Biochim. Pol. 60 (2013) 331–338.

[25] D. Liu, X.Y. Qiu, X. Wu, D.X. Hu, C.Y. Li, S.Bin Yu, F. Pan, X.Q. Chen, Piperlongumine suppresses bladder cancer invasion via inhibiting epithelial mesenchymal transition and F-actin reorganization, Biochem. Biophys. Res. Commun. 494 (2017) 165–172 https://doi.org/10.1016/j.bbrc.2017.10.061.

[26] M. Luty, E. Kwiecień, M. Firlej, A. Łabędź-Masłowska, M. Paw, Z. Madeja, J. Czyz, Curcumin augments the cytostatic and anti-invasive effects of mitoxantrone on carcinosarcoma cells in vitro, Acta Biochim. Pol. 63 (2016) 397–401 https://doi.org/10.18388/abp.2016_1314.

[27] D. Ma, T. Gilbert, C. Pignanelli, D. Tarade, M. Noel, F. Mansour, M. Gupta, S. Ma, J. Ropat, C. Curran, S. Vshyvenko, T. Hudlicky, S. Pandey, Exploiting mitochondrial and oxidative vulnerabilities with a synthetic analog of pancratistatin in combination with piperlongumine for cancer therapy, Faseb. J. 32 (2018) 417–430 https://doi.org/10.1096/fj.201700275R.

[28] Z. Madeja, K. Miękus, J. Sroka, M.B.A. Djamgoz, W. Korohoda, Homotypic cell-cell contacts stimulate the motile activity of rat prostate cancer cells, BJU Int. 88 (2001) 776–786 https://doi.org/10.1046/j.1464-410X.2001.02349.x.

[29] G. Madhavi Sastry, M. Adzhigirey, T. Day, R. Annabhimoju, W. Sherman, Protein and ligand preparation: parameters, protocols, and influence on virtual screening enrichments, J. Comput. Aided Mol. Des. 27 (2013) 221–234 https://doi.org/10.1007/s10822-013-9644-8.

[30] M.J. Meegan, S. Nathwani, B. Twamley, D.M. Zisterer, N.M. O'Boyle, Piperlongumine (piplartine) and analogues: antiproliferative microtubule-destabilising agents, Eur. J. Med. Chem. 125 (2017) 453–463 https://doi.org/10.1016/j.ejmech.2016.09.048.

[31] S. Park, J.H. Kim, Y.Il Hwang, K.S. Jung, Y.S. Jang, S.H. Jang, Schedule-dependent effect of epigallocatechin-3-gallate (EGCG) with paclitaxel on H460 cells, Tuberc. Respir. Dis. 76 (2014) 114–119 https://doi.org/10.4046/trd.2014.76.3.114.

[32] K. Patel, N. Chowdhury, R. Doddapaneni, C.H.A. Boakye, C. Godugu, M. Singh, Piperlongumine for enhancing oral bioavailability and cytotoxicity of docetaxel in triple-negative breast cancer, J. Pharmacol. Sci. 104 (2015) 4417–4426 https://doi.org/10.1002/jps.24637.

[33] R. Petrioli, A.I. Fiaschi, E. Francini, A. Pascucci, G. Francini, The role of doxorubicin and epirubicin in the treatment of patients with metastatic hormone-refractory prostate cancer, Cancer Treat Rev. 34 (8) (2008) 710–718 https://doi.org/10.1016/j.ctrv.2008.05.004.

[34] E.S. Pilka, F.H. Niesen, W.H. Lee, Y. El-Hawari, J.E. Dunford, G. Kochan, V. Wsol, H.J. Martin, E. Maser, U. Oppermann, Structural basis for substrate specificity in human monomeric carbonyl reductases, PLoS One 4 (2009), https://doi.org/10.1371/journal.pone.0007113.

[35] K. Piska, P. Koczurkiewicz, A. Bucki, K. Wójcik-Pszczoła, M. Kołaczkowski, E. Pękala, Metabolic carbonyl reduction of anthracyclines — role in cardiotoxicity and cancer resistance. Reducing enzymes as putative targets for novel cardioprotective and chemosensitizing agents, Invest. N. Drugs 35 (2017), https://doi.org/10.1007/s10637-017-0443-2.

[36] L. Raj, T. Ide, A.U. Gurkar, M. Foley, M. Schenone, X. Li, N.J. Tolliday, T.R. Golub, S.A. Carr, A.F. Shamji, A.M. Stern, A. Mandinova, S.L. Schreiber, S.W. Lee, Selective killing of cancer cells by a small molecule targeting the stress response to ROS, Nature 475 (2011) 231–234 https://doi.org/10.1038/nature10167.

[37] R.W. Robey, K.M. Pluchino, M.D. Hall, A.T. Fojo, S.E. Bates, M.M. Gottesman, Revisiting the role of ABC transporters in multidrug-resistant cancer, Nat. Rev. Canc. (2018) 1–13 https://doi.org/10.1038/s41568-018-0005-8.

[38] S. Goto, Y. Ihara, Y. Urata, S. Izumi, K. Abe, T. Koji, T. Kondo, Doxorubicin-induced DNA intercalation and scavenging by nuclear glutathione S-transferase pi, Faseb. J. 15 (2001) 2702–2714 https://doi.org/10.1096/fj.01-0376com.

[39] O. Tacar, P. Sriamornsak, C.R. Dass, Doxorubicin: an update on anticancer molecular action, toxicity and novel drug delivery systems, J. Pharm. Pharmacol. 65 (2) (2013) 157–170 https://doi.org/10.1111/j.2042-7158.2012.01567.x.

[40] M. Tanaka, R. Bateman, D. Rauh, E. Vaisberg, S. Ramachandani, C. Zhang, K.C. Hansen, A.L. Burlingame, J.K. Trautman, K.M. Shokat, C.L. Adams, An unbiased cell morphology-based screen for new, biologically active small molecules, PLoS Biol. 3 (2005) 0764–0776 https://doi.org/10.1371/journal.pbio.0030128.

[41] S. Thongsom, W. Suginta, K.J. Lee, H. Choe, C. Talabnin, Piperlongumine induces G2/M phase arrest and apoptosis in cholangiocarcinoma cells through the ROS-JNK-ERK signaling pathway, Apoptosis 22 (2017) 1473–1484 https://doi.org/10.1007/s10495-017-1422-y.

[42] C.F. Thorn, C. Oshiro, S. Marsh, T. Hernandez-Boussard, H. McLeod, T.E. Klein, R.B. Altman, Doxorubicin pathways: pharmacodynamics and adverse effects, Pharmacogenetics Genom. 21 (2011) 440–446 https://doi.org/10.1097/FPC.0b013e32833ffb56.

[43] Y. Wang, X. Wu, Y. Zhou, H. Jiang, S. Pan, B. Sun, Piperlongumine suppresses growth and sensitizes pancreatic tumors to gemcitabine in a xenograft mouse model by modulating the NF-kappa B pathway, Cancer Prev. Res. 9 (2016) 234–244 https://doi.org/10.1158/1940-6207.CAPR-15-0306.

[44] X.X. Xiong, J.M. Liu, X.Y. Qiu, F. Pan, S.Bin Yu, X.Q. Chen, Piperlongumine induces apoptotic and autophagic death of the primary myeloid leukemia cells from patients via activation of ROS-p38/JNK pathways, Acta Pharmacol. Sin. 36 (2015) 362–374 https://doi.org/10.1038/aps.2014.141.

[45] Y. Yao, Y. Sun, M. Shi, D. Xia, K. Zhao, L. Zeng, R. Yao, Y. Zhang, Z. Li, M. Niu, K. Xu, Piperlongumine induces apoptosis and reduces bortezomib resistance by inhibiting STAT3 in multiple myeloma cells, Oncotarget 7 (2016) 73497–73508.

[46] F. Zhou, G. Hao, J. Zhang, Y. Zheng, X. Wu, K. Hao, F. Niu, D. Luo, Y. Sun, L. Wu, W. Ye, G. Wang, Protective effect of 23-hydroxybetulinic acid on doxorubicin-induced cardiotoxicity: a correlation with the inhibition of carbonyl reductase-mediated metabolism, Br. J. Pharmacol. 172 (2015) 5690–5703 https://doi.org/10.1111/bph.12995.